Abiotic factors modulate interspecies competition mediated by the type VI secretion system effectors in *Vibrio cholerae*

Running title: Abiotic factors dictate effector effectiveness

Ming-Xuan Tang[1], Tong-Tong Pei[1], Zeng-Hang Wang[1], Han Luo[1], Xing-Yu Wang[1], Tao G. Dong[1, 2*]

Affiliations:

[1] State Key Laboratory of Microbial Metabolism, Joint International Research Laboratory of Metabolic & Developmental Sciences, School of Life Sciences and Biotechnology, Shanghai Jiao Tong University, Shanghai, 200240, China

[2] Department of Ecosystem and Public Health, University of Calgary, 3330 Hospital Dr. NW, Calgary, AB, T2N4Z6, Canada.

[*] Correspondence to tdong@ucalgary.ca

Keywords: protein secretion, interspecies interaction, effector, cation, adaptation

Subject Categories: Microbe-microbe and microbe-host interactions

1 **Abstract**

2   *Vibrio cholerae*, the etiological pathogen of cholera, relies on its type VI secretion system (T6SS) as an

3 effective weapon to survive in highly competitive communities. The anti-bacterial and anti-eukaryotic functions

4 of T6SS depend on its secreted effectors that target multiple essential cellular processes. However, the mechanisms

5 that account for effector diversity and different effectiveness during interspecies competition remain elusive. Here,

6 we report that environmental cations and temperature play a key role in dictating effector-mediated competition

7 of *Vibrio cholerae*. We found that *V. cholerae* could employ its cell-wall-targeting effector TseH to outcompete

8 the otherwise resistant *Escherichia coli* and the *V. cholerae* immunity deletion mutant $\Delta tsiH$ when Ca^{2+} and Mg^{2+}

9 were supplemented. The *E. coli* $\Delta phoQ$ mutant was more sensitive to TseH-mediated killing during competition,

10 suggesting the metal-sensing PhoPQ two-component system is protective to *E. coli* from TseH activity. Using

11 transcriptome analysis, we found multiple stress response systems, including acid stress response, oxidative stress

12 response, and osmotic stress response, were activated in *E. coli* expressing TseH in comparison with *E. coli*

13 expressing the inactive mutant TseH^{H64A}. The membrane-targeting lipase effector TseL also exhibited reduced

14 killing against *E. coli* when divalent cations were removed. In addition, competition analysis of *E. coli* with *V.*

15 *cholerae* single-effector active strains reveals a temperature-dependent susceptibility of *E. coli* to effectors, VasX,

16 VgrG3, and TseL. These findings suggest that abiotic factors, that *V. cholerae* frequently encounters in natural

17 habitats, play a crucial role in dictating the competitive fitness conferred by the type VI secretion system in

18 complex multispecies communities.

19   **Introduction**

20   Living in complex natural and host environments, microbes frequently compete for limited nutrients and

21   ecological niches. To survive, microbes have evolved multiple effective weapons [1–4], one of which is the type

22   VI protein secretion system (T6SS) commonly found in gram-negative bacteria [5–7]. The T6SS consists of three

23   structural parts, a bacteriophage-like baseplate (TssEFGK), a transmembrane complex (TssJLM), and a

24   contractile-tube structure with the Hcp inner tube surrounded by VipA/VipB outer sheath [8–11]. The top of the

25   T6SS Hcp tube is sharpened by a VgrG trimer-PAAR spike complex [12–14]. Upon sheath contraction, the T6SS

26   could inject the inner tube-spike components and the associated effectors directly into the recipient cells [15–17].

27   The physical puncture of T6SS injection causes little harm to recipient cells and it is the T6SS effectors

28   that mainly dictate the T6SS function [17–20]. Effectors are T6SS-secreted toxins exhibiting anti-bacterial and/or

29   anti-eukaryotic activities, and the anti-bacterial effectors mainly include cell-wall disrupting effectors, membrane

30   targeting lipases and pore-forming toxins, nucleases, and cytosolic toxins including $NAD(P)^+$ hydrolase [21],

31   ADP-ribosyl transferase [22], (p)ppApp synthetase [23]. To confer self-protection against anti-bacterial toxins,

32   bacteria encode effector-cognate immunity proteins that specifically interact with effectors [24–27]. In contrast to

33   the specific immunity protein-mediated protection, the innate-immunity-like stress response pathways also provide

34   critical protection against effectors and T6SS delivery, including production of extracellular polysaccharides [18,

35   28], oxidative stress response [29, 30], envelope stress responses [18], acid and osmotic stress response [19]. In

36   addition, spatial separation at the community level can also protect susceptible cells from T6SS aggressors [31–

37   35].

38   T6SS species often encode multiple effector modules which may be used synergistically toward certain

39   species or independently for killing of a broad spectrum of competitors [36–39]. However, some effectors are

40   inactive under lab conditions. For example, in the cholera-causing pathogen *Vibrio cholerae*, the cell-wall targeting

41   trans-peptidase TseH shows little toxicity against *Escherichia coli* or the *V. cholerae* immunity gene deletion

42   mutant Δ*tsiH* when it is delivered by the T6SS [18, 40]. However, TseH is highly toxic to *Aeromonas* and other

43   waterborne species that *V. cholerae* may encounter in the natural environments [18]. Similarly, the lipase effector

44   TseL of *V. cholerae* could be secreted by the T6SS to kill the immunity gene mutant Δ*tsiV1* but it is not very

45 effective against the *E. coli* prey [17, 19, 27]. The difference in susceptibility has been attributed to the nonspecific

46 stress response mechanisms in diverse bacteria [18–20].

47 In this study, we report that a number of abiotic environmental factors, including cations, temperatures

48 and antibiotics, also play a crucial role in T6SS-mediated interspecies competition by modulating target-species

49 sensitivity to specific effectors. Using a panel of single-effector active *V. cholerae* V52 mutants [17, 18], we

50 show that trace amounts of divalent cations, Mg^{2+} and Ca^{2+}, could stimulate TseH toxicity against *E. coli* when

51 delivered by the T6SS, and EDTA treatment abolished such stimulation. The *V. cholerae* Δ*tsiH* mutant was also

52 more sensitive to TseH during competition when Ca^{2+} was supplemented. We further show that deletion of

53 *phoQ*, encoding the sensor of the key two-component system PhoPQ that senses low Mg^{2+} [41], renders *E. coli*

54 more sensitive to TseH-mediated killing, while a constitutively active PhoQ^{D179L} is more resistant. Transcriptome

55 analysis of *E. coli* expressing TseH or its catalytic mutant TseH^{H64A} in the periplasm shows a global cellular

56 change involving multiple pathways, including acid stress response, oxidative stress response, and osmotic stress

57 response, which might be crucial for survival against TseH toxicity. The toxicity of TseL, a lipase effector in *V.*

58 *cholerae*, was also modulated by divalent cations since EDTA treatment resulted in significantly reduced *E. coli*

59 killing mediated by TseL. In addition to cations, *V. cholerae* effectors, VasX, VgrG3 and TseL, also show

60 temperature-dependent toxicity when delivered individually to *E. coli*. Collectively, our data indicate effector-

61 mediated toxicities are modulated by these abiotic factors, highlighting the complex effects of natural

62 environments on interspecies interactions mediated by the T6SS.

63

64 **Results**

65 **T6SS-delivered TseH is conditionally toxic to *E. coli* depending on agar sources.**

66 We have previously reported that the *V. cholerae tseH*$^+$ only mutant, lacking all the other antibacterial

67 effectors, could not outcompete *E. coli* due to the non-specific protections conferred by the envelope stress

68 response pathways [18]. However, we serendipitously found that TseH toxicity was largely affected by the source

69 of agars used for competition. When agar source 1 was used, we reproduced the earlier observation and showed

70 that survival of *E. coli* competed with the *tseH*$^+$ only mutant was comparable to that competed with the T6SS-null

71 mutant Δ*vasK* and the four-effector inactive mutant *4eff$_c$* (Figure 1A, Supplementary Figure 1A). However, when

72   a different source of agar was used (source 2), we noticed that *E. coli* survival was reduced by 10,000-fold in

73   competition with the *V. cholerae tseH*[+] only mutant, relative to that competed with the *4eff$_c$* and $\Delta vasK$ mutant.

74   Survival of *E. coli* remained the same under both agar conditions for samples competed with wild-type *V. cholerae*,

75   the $\Delta vasK$, or the *4eff$_c$* mutant, separately.

76   **Mg^{2+} and Ca^{2+} stimulate TseH-mediated killing against *E. coli*.**

77   To determine the difference between agars that may account for the TseH killing efficiency, we first used

78   XRF (X-Ray Fluorescence) to compare element contents in these two agar samples. XRF results show that Ca and

79   Mg content were substantially higher in source 2 agar (Supplementary Table 1). Using ICP-MS (Inductively

80   Coupled Plasma Mass Spectrometry), we further quantified Mg and Ca content. The Mg and Ca content were

81   85.83±2.40 mg/kg and 16.92±0.30 mg/kg respectively in source 1 agar. However, in source 2 agar, the Mg and Ca

82   content were 515.29±13.57 mg/kg and 200.93±9.29 mg/kg (Table 1), about 6-fold and 10-fold higher than their

83   levels in source 1 agar, respectively.

84   To test if the observed high levels of Mg and Ca are responsible for the enhanced TseH-mediated killing

85   against *E. coli*, we supplemented Mg^{2+} or Ca^{2+} in source 1 agar to the detected levels and tested their effects on

86   bacterial competition. Indeed, the addition of Mg^{2+} or Ca^{2+} stimulated TseH-mediated killing and reduced *E. coli*

87   survival significantly, with Ca^{2+} showing a stronger effect (Figure 1B, Supplementary Figure 1B). Notably, the

88   combination of 0.27 mM Mg^{2+} and 0.07 mM Ca^{2+}, the amount closely resembling the detected levels in source 2

89   agar (Table 2), did not fully reduce *E. coli* survival to that in source 2 agar, suggesting other factors in source 2

90   also contribute to the increased TseH toxicity.

91   To further confirm that metal ions play a critical role in stimulating TseH-mediated killing against *E. coli*,

92   we washed the source 2 agar powder with a metal-chelator EDTA solution to remove divalent cations. Results

93   showed that EDTA-washed source 2 agar failed to support TseH-mediated killing, while the deionized water

94   (ddH$_2$O)-treated source 2 agar could still stimulate TseH killing (Figure 1C, Supplementary Figure 1C). Both the

95   EDTA-treatment and water-treatment did not support TseH-mediated killing on source 1 agar plates.

96   Finally, we also used the defined M9 medium for competition between the *tseH*[+] mutant and *E. coli*. Both

97   M9 with source 1 agar and source 2 agar plates supported TseH-mediated killing, with the source 2 agar plate

98   showing a stronger effect (Figure 1D, Supplementary Figure 1D). Because the M9 salt contains Mg^{2+} and Ca^{2+}(1.0

5

99   mM Ca^{2+}, 0.1 mM Mg^{2+}), we also tested the effects when these two cations were omitted. Results showed that

100   only source 2 agar supported the TseH-mediated killing. Collectively, these results demonstrated that TseH-

101   mediated toxicity is largely dependent on environmental Mg^{2+} and Ca^{2+} levels.

102   **Conditional toxicity of TseH is also appliable to *V. cholerae*.**

103   We have previously reported that deletion of *tseH* cognate immunity gene, *tsiH*, did not render the *V.*

104   *cholerae* mutant susceptible to TseH [40], which is attributed to protection by immunity-independent defense

105   mechanisms, such as the WigKR two-component system [18]. Since *E. coli* showed different sensitivity against

106   TseH with or without Mg^{2+} and Ca^{2+}, we asked whether the *V. cholerae* Δ*tsiH* mutant would be sensitive to TseH

107   in the presence of these two cations. We constructed a Δ*tsiH* deletion mutant lacking the *paar2-tseH-tsiH* three-

108   gene operon in the *4eff_c* mutant background and used it as prey for competition against the *tseH⁺* strain or the *4eff_c*

109   strain, separately. The competition assay results showed that, like *E. coli*, the Δ*tsiH* mutant was sensitive to the

110   *tseH⁺* strain on source 2 agar plates but not on source 1 agar plates, exhibiting a 10-fold reduced survival relative

111   to that exposed to the *4eff_c* killer strain (Figure 1E, Supplementary Figure 1E). In addition, supplementation of 0.3

112   mM Ca^{2+} to source 1 agar reduced the Δ*tsiH* mutant survival significantly, while a combination of 0.27 mM Mg^{2+}

113   and 0.07 mM Ca^{2+} or 0.3 mM Mg^{2+} alone had minor effects. Thus, Ca^{2+} also stimulated TseH-mediated killing

114   against the *V. cholerae* Δ*tsiH* mutant.

115   **The addition of Mg^{2+} and Ca^{2+} does not affect T6SS secretion.**

116   Intrigued by the stimulating effect of Mg^{2+} and Ca^{2+} on TseH-mediated killing, we first hypothesized that

117   Mg^{2+} and Ca^{2+} may affect T6SS secretion efficiency. Thus, we compared the secretion of Hcp with or without

118   Mg^{2+} and Ca^{2+} as an indicator for T6SS activities. The results showed that Hcp was secreted to the same levels

119   with or without Mg^{2+} and Ca^{2+} supplementation between wild type or the *tseH⁺* samples, suggesting the addition

120   of Mg^{2+} and Ca^{2+} has little effect on the T6SS secretion (Figure 2A, Supplementary Figure2A).

121   Next we tested whether TseH requires Mg^{2+} and Ca^{2+} for its activity. TseH is shown to be inactive *in vitro*,

122   and the structural analysis reveals that a short loop might block substrate entry [18]. Therefore, we used an *in vivo*

123   assay by testing TseH toxicity in sensitive prey *A. dhakensis* [18]. Results showed that, with and without Mg^{2+}

124   and Ca^{2+}, the survival of *A. dhakensis* was equally reduced about 2-logs by the *tseH⁺* strain (Figure 2B,

125   Supplementary Figure 2B), relative to that competed with the *4eff_c* and Δ*vasK* mutant, suggesting that TseH

6

126   toxicity is independent of Mg^{2+} and Ca^{2+}. Taken together, these results indicated that the metal-dependent

127   sensitivity of *E. coli* to TseH was not caused by difference in *V. cholerae* T6SS secretion nor changed TseH

128   activities under these two conditions.

129   **PhoPQ two-component system contributes to immunity-independent defense against TseH.**

130   Next, we tested whether sensitivity to TseH results from metal-related defense response in *E. coli*. The

131   PhoPQ two-component system is a key regulatory system and activated in response to Mg^{2+} starvation in *E. coli*

132   [42, 43]. Since the TseH-mediated killing was only observed at high Mg^{2+} / Ca^{2+} levels, we speculated that the

133   PhoPQ system is involved in modulating TseH-killing effects. Specifically, under low Mg^{2+} conditions, the PhoPQ

134   may be activated to confer protection against TseH, while the supplement of Mg^{2+} represses such protection.

135   To test this hypothesis, we constructed the *E. coli* Δ*phoQ* deletion mutant by homologous recombination

136   and used competition assay to compare its survival against the *tseH*[+] strain. Results showed that the deletion of

137   *phoQ* made *E. coli* significantly more sensitive to TseH even in the absence of Mg^{2+} and Ca^{2+} (Figure 3A,

138   Supplementary Figure 3A). We observed a less than one-log survival difference between *E. coli* wild-type and the

139   Δ*phoQ* strains when competed with the *tseH*[+] mutant with Mg^{2+} and Ca^{2+}. We also constructed the *E. coli phoQ*[D179L]

140   strain, a PhoQ locked-on mutant that constitutively phosphorylates PhoP and activates its regulon genes [44].

141   Competition analysis showed that this *phoQ*[D179L] mutation significantly increased *E. coli* survival relative to the

142   Δ*phoQ* with or without Mg^{2+} and Ca^{2+} (Figure 3A). These results suggest that the PhoPQ two-component system

143   also contribute to immunity-independent defense mechanism against TseH toxicities, in addition to the known

144   envelope stress response systems [18].

145   **Transcriptome analysis in *E. coli* periplasmically expressing TseH and its inactive mutant TseH**[H64A]

146   Next, we examined the effect of adding metal cations to *E. coli* using RNA-seq transcriptome analysis.

147   By transferring and incubating exponential-phase-growing *E. coli* to LB source-1-agar plates with and without 0.3

148   mM Mg^{2+} for 30 min prior to RNA extraction, a condition mimicking competition assays, we found very few

149   significant changes for the transcriptomes under these two conditions (Supplementary Figure 3B, Dataset 1). Then,

150   we examined the effect of TseH toxicity on transcriptome expression by ectopically expressing Tat-TseH and its

151   inactive mutant Tat-TseH[H64A] using arabinose-inducible pBAD vectors in *E. coli*. First, we established the

152   induction condition to be 30-min so that the survival of *E. coli* was reduced by TseH to 14.5% of the *E. coli*

153 survival expressing the non-toxic mutant (Figure 3B), suggesting TseH was expressed in most cells. Under this

154 condition, we performed RNA extraction and performed transcriptome analysis. To identify genes differentially

155 expressed, we set the cut-off value of fold change > 1.5 and p-value < 0.05. We also removed the low transcriptome

156 gene with an average FPKM (fragments per kilobase per million mapped fragments) < 10. By comparing the

157 transcriptome of these two strains, we found 106 genes were differentially expressed, of which 50 genes were up-

158 regulated and 56 genes were down-regulated (Figure 3C, Supplementary Figure 3C, Dataset 2).

159   Among the up-regulated genes, 22 genes belonged to the RpoS general stress response regulon, including

160 *gadCF* and *osmY* (Figure 3D). We also found three small regulatory RNA, *gadF*, *glmY* and *omrB* were up-

161 regulated. *GadF* is involved in acid stress response [45, 46]; *GlmY* controls the amino sugar metabolism in *E. coli*

162 by post-transcription and deletion of *glmY* renders cells sensitive to envelope stress [47]. *OmrB* is a small RNA

163 that is involved in regulating the protein composition of the outer membrane [48]. Among the down-regulated

164 genes, we found 24 genes belonging to the heat-shock response RpoH regulon were down-regulated, including

165 *dnaK*, *groL*, *groS*, and the protease gene *lon*. These genes are important for proper protein folding.

166   We have shown that the T6SS delivered-TseH induces the envelope stress response in *E. coli* [18]. In the

167 transcriptome results, we found the BaeR regulon gene *ycaC* was up-regulated. In addition, *gadF*, also a PhoPQ-

168 regulated gene, was upregulated. Another PhoPQ-regulated gene *mgrB*, involved in Mg^{2+} uptake, was up-regulated

169 with p-value<0.05 but with a moderate fold change <1.5.

170   To validate the RNA-seq data, we performed qRT-PCR assays of 14 genes, of which 7 were up-regulated

171 and 7 were down-regulated. These genes were with the relative high fold change in RNA-seq results. The 16S

172 rRNA gene was used as the reference. The qRT-PCR results were consistent with the RNA-seq results (Figure

173 3E).

174 **Divalent cations contribute to TseL-mediated toxicity.**

175   We also noticed that another T6SS effector TseL with phospholipase activity in *V. cholerae*, also exhibited

176 different toxicity against *E. coli* on different agar sources during interspecies competition. On source 1 agar plates,

177 the *V. cholerae tseL*+ mutant reduced *E. coli* survival by 100-fold relative to the *4effc* mutant. In contrast, on source

178 2 agar plates, the *E. coli* survival was reduced about 10,000-fold by the *tseL*+ mutant relative to the *4effc* mutant

179 (Figure 4A, Supplementary Figure 4A). In addition, EDTA-treatment of different agar sources also abolished

8

180   TseL-mediated killing difference between the two agar sources (Figure 4B, Supplementary Figure 4B). When

181   comparing *E. coli* survival on TseL-sensitive agar source 2, we found that EDTA-treatment increased *E. coli*

182   survival by 100-fold relative to deionized water-treatment. To further investigate which divalent cations play a

183   role in this process, we competed the *tseL*+ mutant and *E. coli* on source 1 agar plates supplemented with 0.3 mM

184   Mg^{2+}, Ca^{2+}, Ni^{2+} and Cu^{2+}, respectively. However, unlike TseH, none of the tested cations increased the TseL-

185   toxicity to the agar source 2 levels (Figure 4C, Supplementary Figure 4C). Nonetheless, these results suggest that

186   TseL-mediated toxicity is also modulated by some EDTA-chelatable divalent cations.

187   **Temperature affects effector-mediated competition.**

188   Since *V. cholerae* may also experience temperature changes in the environment or during transmission

189   from environment to the host, we next determined whether temperature also plays a role in effector-mediated

190   bacterial competition. We used a panel of *V. cholerae* single-effector-active killer strains and *E. coli* as prey.

191   Results show that the relative survival of *E. coli* was significantly reduced at 30 ℃ in comparison to that at 37 ℃

192   when *E. coli* was competed with the *vasX*+ (with membrane pore-forming activity) and the *vgrG3*+ (a lysozyme)

193   strains, separately (Figure 4D, Supplementary Figure 4D). In contrast, the survival of *E. coli* was significantly

194   increased at 30 ℃ relative to that at 37 ℃ when *E. coli* was competed with the *tseL*+ strain (Figure 4D,

195   Supplementary Figure 4D). These results collectively indicate that temperature also plays an important role in

196   T6SS-mediated competition.

197   **VasX-toxicity in *P. aeruginosa* is dependent on temperature and the antibiotic irgasan.**

198   We have previously reported that periplasmic expression of VasX using a Tat secretion signal is highly

199   toxic in *E. coli* but not in *Pseudomonas aeruginosa* PAO1, an important opportunistic pathogen [19]. We thus

200   tested whether the resistance of *P. aeruginosa* to VasX is also temperature-dependent. First, we confirmed this

201   resistance phenotype by comparing the survival of PAO1 expressing plasmid-borne Tat-VasX or its inactive

202   mutant Tat-VasX$^{\Delta C16}$ [17] at 37 ℃ (Figure 4E). However, when VasX was highly induced at 30 ℃, we found that

203   survival of PAO1 was reduced to undetectable levels (Figure 4E). Because the assays were performed on plates

204   containing two antibiotics, irgasan that PAO1 is intrinsically resistant to, and gentamycin whose resistance is

205   conferred by the pTat-VasX plasmid, and because expression of VasX increases membrane permeability [19], we

206   hypothesized that the increased sensitivity to VasX may be caused by the presence of antibiotics. We repeated

9

207 periplasmic expression of VasX in PAO1 but only plated the induced cells on gentamycin. We found that PAO1

208 became resistant to VasX expression at both 30 ℃ and 37 ℃ (Supplementary Figure 4E). These results suggest

209 that the membrane damages caused by VasX expression at 30 ℃, albeit insufficient to cause cell death directly,

210 can disturb the intrinsic resistance of *P. aeruginosa* to irgasan (Figure 4E, Supplementary Figure 4E).

211

212 **Discussion**

213 Microbes have been found in almost all ecological niches on earth and contribute to a variety of functions

214 ranging from macroscale carbon recycling and waste removal to individual-level host health and disease. These

215 functions are often determined by not a single but multiple species that coexist in complex communities, with

216 extensive interspecies interactions via various molecular mechanisms. The T6SS is one such crucial mechanism

217 exhibiting anti-bacterial, anti-fungal and other anti-eukaryotic functions [5, 24, 49–51]. From a molecular

218 ecological perspective, the T6SS-mediated interspecies competition is a complex and multifaced process whose

219 outcome is determined by diverse factors including the number and type of the secreted effectors [31], the

220 frequency of T6SS firing correlated with energy state [31], the immunity protein-dependent specific protection

221 [24], the non-specific stress response pathways in killer and prey cells [18, 20], and the availability of nutrients

222 [52][53]. Here, we add on to this list by showing that abiotic environmental factors can modulate prey cell

223 sensitivity to effector toxicities, thereby affecting T6SS-mediated competition (Figure 6). Our results demonstrate

224 not only that some seemingly inactive effectors may be highly toxic in natural settings but also the importance of

225 examining toxin-mediated interspecies interactions beyond the routine lab conditions.

226 Almost all T6SS species secrete multiple effectors with obvious benefits for T6SS-mediated competitive

227 fitness [31, 37, 39]. However, many effectors are phenotypically inactive, hindering the full understanding of the

228 ecological functions of the T6SS. An elegant strategy employing barcoding-sequencing analysis of mixed effector-

229 susceptible populations in *P. aeruginosa* reveals that effectors may act jointly with other effectors to exert

230 synergistic functions but their activities can also be variable depending on salinity, pH and aerobic conditions [39].

231 Here we show the ecologically-relevant abiotic factors, including cations and temperature, that microbes

232 frequently encounter in nature environment, play a critical role in mediating T6SS-dependent interspecies killing.

233 Our previous study on the *V. cholerae* T6SS effector TseH reveals that *E. coli* mutants impaired in envelope stress

234   response (ESR) pathways, but not the wild type, are sensitive to TseH toxicities [18]. Here we show that

235   supplementation of Mg^{2+} and Ca^{2+} cations can render *E. coli* susceptible to TseH despite of the intact ESR

236   protection. Another effector TseL has also exhibited cation-related toxicity since EDTA-treatment of the agar

237   could reduce TseL-mediated killing against *E. coli*. Notably, as *V. cholerae* is a waterborne pathogen commonly

238   found in water sources in which Mg^{2+} (average concentration 50 mM) and Ca^{2+} (~ 10 mM) are present at much

239   higher levels than the levels supplemented here [54], the *V. cholerae* T6SS effectors may have a broader target

240   range in the natural niche. Indeed, when a source of raw agar was used, we also found highly increased TseH-

241   mediated killing against *E. coli* (Figure 5A, 5B, Supplementary Figure 5A, 5B).

242   Mg^{2+} and Ca^{2+} are known to have critical cellular functions, but the effect of cations on T6SS effector

243   toxicities in prey cells has not been reported before. As the most abundant divalent cation in living cells, Mg^{2+}

244   neutralizes the negative charge of biomolecules, including nucleotides and nucleic acids, phospholipids in various

245   membrane structures in cells, as well as serving as an indispensable cofactor in various enzymes [41, 55, 56]. Like

246   Mg^{2+}, Ca^{2+} could also maintain cell structure, participate in motility and cell division processes [57, 58]. Due to

247   the critical role Mg^{2+} and Ca^{2+} play in bacteria, the concentrations of Mg^{2+} and Ca^{2+} are tightly regulated [56, 59].

248   Under low Mg^{2+} conditions, the two component system PhoPQ is activated to regulate a large number of genes

249   involved in virulence, metal uptake, and other important functions [41, 56]. The increased resistance of *E. coli* to

250   TseH in agar source 1 with lower Mg^{2+} may thus be attributed to activation of PhoPQ. Indeed, deletion of *phoQ*

251   leads to increased sensitivity to TseH, suggesting that the PhoPQ-system is important for such protection (Figure

252   3A).

253   Although we have yet to determine the exact physiological changes in prey cells that account for the

254   temperature and cation-dependent effector-mediated competition, it is likely a multifaceted process that involves

255   a number of different cellular pathways, as exemplified in the transcriptome changes upon TseH induction (Figure

256   3C, 3D). Given the prevalence of T6SS organisms, including plant and host pathogens, as well as the diversity of

257   effectors in each species, it is crucial to take into account of ecologically relevant conditions for testing T6SS-

258   related effector functions and interspecies interactions in future studies. The environmental cues, such as cations

259   and temperature, may have profound effects on the composition of T6SS-containing microbial communities and

260   the evolution of their defense and attack mechanisms.

261

262 **Methods**

263 **Strains and growth conditions**

264   Strains and plasmids used in this study are described in Supplementary Table 2. All constructs were verified

265 by sequencing. Primers are available in Dataset 3. Bacteria were grown in LB([w/v] 1% tryptone, 0.5% yeast

266 extract, 0.5% NaCl) at 37 ℃ aerobically. Antibiotics and inducers were used at following concentrations:

267 kanamycin (25 µg/mL for *E. coli*, 50 µg/mL for *V. cholerae* and *A. dhakensis*), streptomycin (100 µg/mL),

268 chloramphenicol (2.5 µg/mL for *V. cholerae* and 25 µg/mL for *E. coli*), irgasan (25 µg/mL), gentamycin (20

269 µg/mL), L-arabinose ([w/v] 0.1% or 0.01% as indicated), IPTG (0.1 mM or 1 mM as indicated). Tryptone (BIO

270 BASIC, TG217(G211)), yeast extract (BIO BASIC, G0961), source 1 agar (BIO BASIC, FB0010), source 2 Agar

271 (Sangon Biotech, A505255-0250).

272 **EDTA treatment of agar powder**

273   Agar powders were washed by 0.1 M EDTA solution for 5 min with vortex, followed by deionized water

274 washing with 5 times to remove EDTA. Then the treated agar was dried and could be used for bacterial competition

275 experiments.

276 **Bacterial competition assay**

277   Competing strains were grown overnight in LB with appropriate antibiotics. Killer cells were then sub-

278 cultured to OD_{600}=1. For interspecies competition, killer and prey cells were mixed at a ratio of 5:1 and co-

279 incubated on LB-agar plates or M9-agar (93.0 mM Na^+, 22.1 mM K^+, 18.7 mM NH_4^+, 1.0 mM Ca^{2+}, 0.1 mM

280 Mg^{2+}, 29.2 mM Cl^-, 0,1 mM SO_4^{2-}, 42.2 mM PO_4^{2-}, [w/v] 0.1% glucose) plates at 37 ℃ or 30 ℃ (as indicated)

281 for 3 h. For intraspecies competition, killer and prey cells were mixed at a ratio of 20:1 and co-incubated on LB-

282 agar plates at 37 ℃ for 20 h (or 3 h when using raw agar). After co-incubation, the survival of killer and prey

283 cells were enumerated by 10-fold serial plating on LB plates with selective antibiotics. The mean Log_{10} c.f.u of

284 the recovered killer and prey strains was plotted and error bars show the mean ± standard deviation of at least

285 three biological replicates. A two-tailed Student's *t*-test and one-way ANOVA test was used to determine *p*-

286 values.

287 **XRF and ICP analysis**

288   XRF (X-Ray Fluorescence) and ICP (Inductively Coupled Plasma Mass Spectrometry) analysis was done

289   by the Instrumental Analysis Center in Shanghai Jiao Tong university. For XRF analysis, the agar powder was

290   pressed into disks (30 mm diameter) and performed with a XRF (XRF-1800, SHIMADZU). For ICP analysis,

291   the two agar samples were digested with 5 mL concentrated nitric acid and diluted to 50 mL with ultrapure

292   water. After samples were prepared, elemental analysis was performed with an ICP (Avio 500, PerkinElmer).

293   **Protein secretion assay**

294   Strains were grown overnight in LB with appropriate antibiotics. Cells were then sub-cultured to $OD_{600}=1$

295   with or without Mg^{2+} and Ca^{2+}. 2 ml of OD_{600} 1 cells were collected by centrifuge at $2,500 \times g$ for 3 min and

296   resuspended in 1 mL fresh LB. Resuspended cells were placed at 30 °C for 1 h and centrifuged at $10,000 \times g$ for

297   2 min at room temperature (RT). Cell pellet was used as the whole-cell sample. The supernatant was centrifuged

298   at $10,000 \times g$ for 2 min again as the secretion sample. All samples were mixed with SDS-loading dye, boiled at

299   98 ℃ for 10 min, followed by SDS-PAGE (sodium dodecyl sulfate polyacrylamide gel electrophoresis) analysis

300   and Western blotting analysis.

301   **Western blotting analysis**

302   After electrophoresis in a 12% SDS-PAGE gel, proteins were transferred to a PVDF membrane (Bio-Rad).

303   Then, the protein-bound membrane was blocked with 5% [w/v] non-fat milk in TBST (50 mM Tris, 150 mM

304   NaCl, 0.1% [v/v] Tween-20, pH 7.6) buffer for 1 h at RT. After blocking, the membrane was sequentially

305   incubated with primary and secondary HRP (horseradish peroxidase)-conjugated antibodies in TBST with 1%

306   [w/v] milk for 1 h at RT. Signals were detected using the Clarity ECL solution (Bio-Rad). The monoclonal

307   antibody to RpoB, the beta subunit of RNA polymerase, were purchased from Biolegend (RpoB, Product #

308   663905). The polyclonal antibody to Hcp was custom-made by Shanghai Youlong Biotech. The HRP-linked

309   secondary antibodies were purchased from ZSGB-Bio (Product # ZB-2305 (mouse) and # ZB-2301 (rabbit)).

310   The Hcp antibody was used at 1:10000 dilution, while others at 1:20000 dilution.

311   **Toxicity assay**

312   For VasX toxicity assay in PAO1, overnight cells carrying pPSV37 constructs were grown in LB with

313   appropriate antibiotics and 0.2% [w/v] glucose at 37 ℃. Cells were then collected and resuspended in fresh LB.

13

314   A serial dilution was plated on LB plates containing 0.1 mM, 1 mM IPTG or 0.2% [w/v] glucose with antibiotics

315   as indicated.

RNA sample preparation

317   For transcriptome analysis of *E. coli* with or without Mg^{2+}, exponential-phase-growing *E. coli* cells were

318   collected and transferred onto LB plates with or without 0.3 mM Mg^{2+} for 30 min prior to RNA extraction. For

319   transcriptome analysis of *E. coli* ectopically expressing Tat-TseH and its inactive mutant Tat-TseH[H64A], *E. coli*

320   strains with pBAD24kan-Tat-TseH/TseH[H64A] plasmid were grown overnight on LB plates with appropriate

321   antibiotics and 0.2% [w/v] glucose. Cells were then sub-cultured to $OD_{600}=1$, collected by centrifugation at

322    $10,000 \times g$ for 0.5 min and washed twice with fresh LB. After being recovered at 37 ℃ for 10 min, cells were

323   induced with 0.1% [w/v] arabinose for 30 min followed by total RNA extraction. The survival of *E. coli* strains

324   after induction was enumerated by 10-fold serial plating on LB plates with selective antibiotics and 0.2% [w/v]

325   glucose.

RNA extraction

327   100 μL 8×lysis buffer (8% [w/v] SDS, 16mM EDTA) was added into 700 μL culture of each sample after

328   induction and mixed well by vortex for 5 s. Then 800 μL prewarmed hot acidic phenol (65 ℃) was added and

329   mixed by inverting immediately. Tubes were incubated at 65 ℃ for 5 min with mixing briefly every 1 min. After

330   putting on ice for 10 min, the mixture was centrifuged at $13,000 \times g$ for 2 min. The top supernatant was carefully

331   transferred to a new tube and an equal-volume of absolute ethanol was added. Then the crude RNA was purified

332   by RNA prep Pure Cell/Bacteria Kit (TIANGEN, Product #DP430) and genomic DNA was removed by DNase I

333   (NEB, Product B0303S) treatment at 37 ℃ for 30 min. After DNase I treatment, RNA samples were then

334   purified with the RNA clean Kit (TIANGEN, Product #DP421). Purified RNA was electrophoresed on 1% [w/v]

335   agarose gel to monitor the integrity and contaminants.

Transcriptome analysis

337   RNA-seq was done by Novogene. Briefly, rRNA was removed from total RNA samples by using probes.

338   Then obtained mRNA was fragmented by divalent cations. The first strand cDNA was synthesized by M-MuLV

339   Reverse Transcriptase using random hexamers as primers. The RNA strand was degraded by RNase H. The

340   second strand of cDNA was synthesized using dUTP to replace dTTP in dNTP mixture. The purified double-

14

341 stranded cDNA was end-repaired, adding an A tail and connecting to the sequencing adapter. USER enzyme

342 (NEB, USA) was used to degrade the second strand of cDNA containing U. After using AMPure XP beads to

343 screen cDNA with 370~420 bp and PCR amplification of these fragments, the final library was obtained with

344 another cycle of AMPure XP beads purification. The clustering of the index-coded samples was performed on a

345 cBot Cluster Generation System following to the manufacturer's instructions, and the sequencing was performed

346 using the Illumina Hiseq TM 2500 platform with pair-end 150 base reads. Raw data was filtered according to the

347 following standards: (1) removing reads with unidentified nucleotides (N); (2) removing reads with low

348 sequencing quality (>50% bases having Phred quality scores of ≤20); (3) removing reads with the adapter. The

349 obtained clean data were used for downstream analysis. Bowtie2-2.2.3 was used to build an index of the

350 reference genome and align clean reads to reference genome. The gene expression level was calculated and

351 further normalized by HTSeq v0.6.1. FPKM, fragments per kilobase of transcript sequence per millions base

352 pairs sequenced, was used to demonstrated gene expression level here.

353 **Bioinformatics Analysis**

354 Differential expression genes were identified by setting cut-off value of fold change > 1.5, p-value < 0.05.

355 and average FPKM > 10. PCA analysis was performed by R package FactoMineR. Person correlation coefficient

356 was calculated by R package WGCNA. Heat map was performed in Origin App: Heat map with Dendrogram.

357 **qRT-PCR Analysis**

358 14 differential expression genes were chosen from transcriptome results. Primers for qPCR were designed

359 by PerlPrimer. The 16S rRNA gene was used as the reference. Reverse transcription was done using

360 PrimeScript™ RT reagent Kit with gDNA Eraser (Perfect Real Time) (Takara, #RR047A). qPCR reaction was

361 prepared by TB Green® Premix Ex Taq™ (Tli RNaseH Plus) (Takara, #RR420A) and detected by CFX Connect

362 Real-Time PCR Detection System (BIO-RAD, #1855201). Analysis of relative gene expression was calculated

363 using the $2^{-\Delta\Delta CT}$ method. Each sample was measured in triplicate and repeated at least three times.

364 **Data availability**

365 The data that support the findings of this study are available within the paper or available from the corresponding

366 author upon reasonable request.

367 **References**

15

1. Chassaing B, Cascales E. Antibacterial weapons: targeted destruction in the microbiota. *Trends Microbiol* 2018; **26**: 329–338.

2. Aoki SK, Pamma R, Hernday AD, Bickham JE, Braaten BA, Low DA. Contact-dependent inhibition of growth in *Escherichia coli*. *Science* 2005; **309**: 1245–1248.

3. Taylor NMI, van Raaij MJ, Leiman PG. Contractile injection systems of bacteriophages and related systems. *Mol Microbiol* 2018; **108**: 6–15.

4. Kohanski MA, Dwyer DJ, Collins JJ. How antibiotics kill bacteria: from targets to networks. *Nat Rev Microbiol* 2010; **8**: 423–435.

5. Pukatzki S, Ma AT, Sturtevant D, Krastins B, Sarracino D, Nelson WC, et al. Identification of a conserved bacterial protein secretion system in *Vibrio cholerae* using the *Dictyostelium* host model system. *Proc Natl Acad Sci U S A* 2006; **103**: 1528–1533.

6. Mougous JD, Cuff ME, Raunser S, Shen A, Zhou M, Gifford CA, et al. A virulence locus of *Pseudomonas aeruginosa* encodes a protein secretion apparatus. *Science (80-)* 2006; **312**: 1526–30.

7. Bingle LE, Bailey CM, Pallen MJ. Type VI secretion: a beginner's guide. *Curr Opin Microbiol* 2008; **11**: 3–8.

8. Basler M, Pilhofer M, Henderson GP, Jensen GJ, Mekalanos JJ. Type VI secretion requires a dynamic contractile phage tail-like structure. 2012.

9. Durand E, Nguyen VS, Zoued A, Logger L, Péhau-Arnaudet G, Aschtgen M-S, et al. Biogenesis and structure of a type VI secretion membrane core complex. *Nature* 2015; **523**: 555–560.

10. Zoued A, Durand E, Brunet YR, Spinelli S, Douzi B, Guzzo M, et al. Priming and polymerization of a bacterial contractile tail structure. *Nature* 2016; **531**: 59–63.

11. Kudryashev M, Wang RYR, Brackmann M, Scherer S, Maier T, Baker D, et al. Structure of the Type VI secretion system contractile sheath. *Cell* 2015; **160**: 952–962.

12. Shneider MM, Buth SA, Ho BT, Basler M, Mekalanos JJ, Leiman PG. PAAR-repeat proteins sharpen and diversify the type VI secretion system spike. *Nature* 2013; **500**: 350–353.

13. Pukatzki S, Ma AT, Revel AT, Sturtevant D, Mekalanos JJ. Type VI secretion system translocates a phage tail spike-like protein into target cells where it cross-links actin. *Proc Natl Acad Sci U S A* 2007; **104**: 15508–15513.

14. Leiman PG, Basler M, Ramagopal UA, Bonanno JB, Sauder JM, Pukatzki S, et al. Type VI secretion apparatus and phage tail-associated protein complexes share a common evolutionary origin. 2009.

15. Vettiger A, Basler M. Type VI secretion system substrates are transferred and reused among sister cells. *Cell* 2016; **167**: 99-110.e12.

16. Ho BT, Fu Y, Dong TG, Mekalanos JJ. *Vibrio cholerae* type 6 secretion system effector trafficking in target bacterial cells. *Proc Natl Acad Sci U S A* 2017; **114**: 9427–9432.

17. Liang X, Kamal F, Pei TT, Xu P, Mekalanos JJ, Dong TG. An onboard checking mechanism ensures effector delivery of the type VI secretion system in *Vibrio cholerae*. *Proc Natl Acad Sci U S A* 2019; **116**: 23292–23298.

18. Hersch SJ, Watanabe N, Stietz MS, Manera K, Kamal F, Burkinshaw B, et al. Envelope stress responses defend against type six secretion system attacks independently of immunity proteins. *Nat Microbiol* 2020; **5**: 706–714.

19. Kamal F, Liang X, Manera K, Pei TT, Kim H, Lam LG, et al. Differential Cellular Response to Translocated Toxic Effectors and Physical Penetration by the Type VI Secretion System. *Cell Rep* 2020; **31**: 107766.

20. Hersch SJ, Manera K, Dong TG. Defending against the Type Six Secretion System: beyond Immunity Genes. *Cell Rep* 2020; **33**: 108259.

21. Whitney JC, Quentin D, Sawai S, LeRoux M, Harding BN, Ledvina HE, et al. An Interbacterial NAD(P)+ Glycohydrolase Toxin Requires Elongation Factor Tu for Delivery to Target Cells. *Cell* 2015; **163**: 607–619.

22. Ting SY, Bosch DE, Mangiameli SM, Radey MC, Huang S, Park YJ, et al. Bifunctional Immunity Proteins Protect Bacteria against FtsZ-Targeting ADP-Ribosylating Toxins. *Cell* 2018; **175**: 1380-1392.e14.

23. Ahmad S, Wang B, Walker MD, Tran HKR, Stogios PJ, Savchenko A, et al. An interbacterial toxin inhibits target cell growth by synthesizing (p)ppApp. *Nature* 2019; **575**: 674–678.

24. Hood RD, Singh P, Hsu F, Güvener T, Carl MA, Trinidad RRS, et al. A type VI secretion system of *Pseudomonas aeruginosa* targets a toxin to bacteria. *Cell Host Microbe* 2010; **7**: 25–37.

25. Russell AB, Hood RD, Bui NK, Leroux M, Vollmer W, Mougous JD. Type VI secretion delivers bacteriolytic effectors to target cells. *Nature* 2011; **475**: 343–349.

26. Brooks TM, Unterweger D, Bachmann V, Kostiuk B, Pukatzki S. Lytic activity of the *Vibrio cholerae* type VI secretion toxin VgrG-3 is inhibited by the antitoxin TsaB. *J Biol Chem* 2013; **288**: 7618–7625.

27. Dong TG, Ho BT, Yoder-Himes DR, Mekalanos JJ. Identification of T6SS-dependent effector and immunity proteins by Tn-seq in *Vibrio cholerae*. *Proc Natl Acad Sci U S A* 2013; **110**: 2623–2628.

28. Toska J, Ho BT, Mekalanos JJ. Exopolysaccharide protects *Vibrio cholerae* from exogenous attacks by the type 6 secretion system. *Proc Natl Acad Sci U S A* 2018; **115**: 7997–8002.

29. Dong TG, Dong S, Catalano C, Moore R, Liang X, Mekalanos JJ. Generation of reactive oxygen species by lethal attacks from competing microbes. *Proc Natl Acad Sci U S A* 2015; **112**: 2181–2186.

30. Storey D, Id AM, Mia Å, Graca J, Id S, Rodriguez-escudero I, et al. *Klebsiella pneumoniae* type VI secretion system-mediated microbial competition is PhoPQ controlled and reactive oxygen species dependent. *PLoS Pathogens* . 2020.

31. Wong MJQQ, Liang X, Smart M, Tang L, Moore R, Ingalls B, et al. Microbial herd protection mediated by antagonistic interaction in polymicrobial communities. *Appl Environ Microbiol* 2016; **82**: 6881–6888.

32. Borenstein DB, Ringel P, Basler M, Wingreen NS. Established Microbial Colonies Can Survive Type VI Secretion Assault. *PLoS Comput Biol* 2015; **11**: 1–16.

33. McNally L, Bernardy E, Thomas J, Kalziqi A, Pentz J, Brown SP, et al. Killing by Type VI secretion drives genetic phase separation and correlates with increased cooperation. *Nat Commun* 2017; **8**: 14371.

34. Cardarelli L, Saak C, Gibbs KA. Two Proteins Form a Heteromeric Bacterial Self-Recognition Complex in Which Variable Subdomains Determine Allele-Restricted Binding. *MBio* 2015; **6**: e00251.

35. Smith WPJ, Vettiger A, Winter J, Ryser T, Comstock LE, Basler M, et al. The evolution of the type VI secretion system as a disintegration weapon. *PLoS Biol* 2020; **18**: 1–26.

36. Russell AB, Peterson SB, Mougous JD. Type VI secretion system effectors: Poisons with a purpose. *Nat Rev Microbiol* 2014; **12**: 137–148.

37. Ho BT, Dong TG, Mekalanos JJ. A view to a kill: the bacterialtype VI secretion system. *Cell Host Microbe* 2014; **15**: 9–21.

38. Jurėnas D, Journet L. Activity, delivery, and diversity of Type VI secretion effectors. *Mol Microbiol* 2020; 1–12.

39. LaCourse KD, Peterson SB, Kulasekara HD, Radey MC, Kim J, Mougous JD. Conditional toxicity and synergy drive diversity among antibacterial effectors. *Nat Microbiol* 2018; **3**: 440–446.

40. Altindis E, Dong T, Catalano C, Mekalanos J. Secretome analysis of *Vibrio cholerae* type VI secretion system reveals a new effector-immunity pair. *MBio* 2015; **6**: e00075-15.

41. García Véscovi E, Soncini FC, Groisman EA. Mg^{2+} as an extracellular signal: environmental regulation of *Salmonella* virulence. *Cell* 1996; **84**: 165–174.

42. Kato A, Tanabe H, Utsumi R. Molecular characterization of the PhoP-PhoQ two-component system in *Escherichia coli* K-12: Identification of extracellular Mg^{2+}-responsive promoters. *J Bacteriol* 1999; **181**: 5516–5520.

43. Minagawa S, Ogasawara H, Kato A, Yamamoto K, Eguchi Y, Oshima T, et al. Identification and molecular characterization of the Mg^{2+} stimulon of *Escherichia coli*. *J Bacteriol* 2003; **185**: 3696–3702.

44. Minagawa S, Okura R, Tsuchitani H, Hirao K, Yamamoto K, Utsumi R. Isolation and molecular characterization of the locked-on mutant of Mg^{2+} sensor PhoQ in *Escherichia coli*. *Biosci Biotechnol Biochem* 2005; **69**: 1281–1287.

45. Melamed S, Peer A, Faigenbaum-Romm R, Gatt YE, Reiss N, Bar A, et al. Global Mapping of Small RNA-Target Interactions in Bacteria. *Mol Cell* 2016; **63**: 884—897.

46. Hommais F, Krin E, Coppée JY, Lacroix C, Yeramian E, Danchin A, et al. GadE (YhiE): A novel activator involved in the response to acid environment in *Escherichia coli*. *Microbiology* 2004; **150**: 61–72.

47. Hobbs EC, Astarita JL, Storz G. Small RNAs and small proteins involved in resistance to cell envelope stress and acid shock in *Escherichia coli*: Analysis of a bar-coded mutant collection. *J Bacteriol* 2010; **192**: 59–67.

48. Guillier M, Gottesman S. Remodelling of the *Escherichia coli* outer membrane by two small regulatory RNAs. *Mol Microbiol* 2006; **59**: 231–247.

49. MacIntyre DL, Miyata ST, Kitaoka M, Pukatzki S. The *Vibrio cholerae* type VI secretion system displays antimicrobial properties. *Proc Natl Acad Sci* 2010; **107**: 19520–19524.

50. Trunk K, Peltier J, Liu YC, Dill BD, Walker L, Gow NAR, et al. The type VI secretion system deploys antifungal effectors against microbial competitors. *Nat Microbiol* 2018; **3**: 920–931.

51. Ma AT, McAuley S, Pukatzki S, Mekalanos JJ. Translocation of a *Vibrio cholerae* Type VI Secretion Effector Requires Bacterial Endocytosis by Host Cells. *Cell Host Microbe* 2009; **5**: 234–243.

52. Yu M, Wang YC, Huang CJ, Ma LS, Lai EM. *Agrobacterium tumefaciens* deploys a versatile antibacterial strategy to increase its competitiveness. *J Bacteriol* 2021; **203**: 1–15.

53. Crisan C V., Nichols HL, Wiesenfeld S, Steinbach G, Yunker PJ, Hammer BK. Glucose confers protection to *Escherichia coli* against contact killing by *Vibrio cholerae*. *Sci Rep* 2021; **11**: 1–11.

54. Mewes A, Langer G, de Nooijer LJ, Bijma J, Reichart G-J. Effect of different seawater Mg^{2+} concentrations on calcification in two benthic foraminifers. *Mar Micropaleontol* 2014; **113**: 56–64.

55. Pontes MH, Sevostyanova A, Groisman EA. When Too Much ATP Is Bad for Protein Synthesis. *J Mol Biol* 2015; **427**: 2586–2594.

56. Groisman EA, Hollands K, Kriner MA, Lee EJ, Park SY, Pontes MH. Bacterial Mg^{2+} homeostasis, transport, and virulence. *Annu Rev Genet* 2013; **47**: 625–646.

57. Smith RJ. Calcium and Bacteria. *Adv Microb Physiol* 1995; **37**: 83–133.

58. Dominguez DC. Calcium signalling in bacteria. *Mol Microbiol* 2004; **54**: 291–297.

59. Gangola P, Rosens BP. Maintenance of Intracellular Calcium in *Escherichia coli*. 1987; **262**: 12570–12574.

368

Competing interests

The authors declare no competing interests.

Author contributions

T.D. conceived the project. M.T. performed most of the experiment and data analysis. T.P., Z.W., and H.L. performed experiments. X.W. contributed to RNA-seq data analysis. M.T. prepared the first draft. T.D. contributed to the revision with assistance from M.T. and T.P..

Correspondence and request for materials should be addressed to T. Dong.

Table 1. Determination of Mg and Ca in agar powder by ICP-MS

	Mg (mg/kg)	Ca (mg/kg)
Agar (Source 1)	85.83±2.40	16.92±0.30
Agar (Source 2)	515.29±13.57	200.93±9.29

Table 2. Content of Mg and Ca in LB plates with 1.3% agar

	Mg (μmol/L)	Ca (μmol/L)
Agar (Source 1)	46.04±1.30	5.50±0.10
Agar (Source 2)	279.16±7.35	65.30±3.02

382

383   **Figure legends**

384   **Figure 1. Mg^{2+} and Ca^{2+} stimulate TseH-mediated killing against *E. coli* and the *V. cholerae* Δ*tsiH* mutant.**

385   **A,** Survival of *E. coli* after competition with *V. cholerae* strains on LB plates of two different agar sources. **B,**

386   Survival of *E. coli* competed with *V. cholerae* strains on LB plates of agar source 1, supplemented with Mg^{2+} and

387   Ca^{2+}. **C,** Effect of EDTA-treatment on survival of *E. coli* competed with *V. cholerae* strains. LB plates of ddH$_2$O-

388   treated agar were used as control. **D,** Survival of *E. coli* competed with *V. cholerae* strains on M9 source-1-agar

389   or source-2-agar plates. **E,** Survival of the *V. cholerae* Δ*tsiH* mutant after competition with the *4eff$_c$* and *tseH$^+$*

390   strain. For **A** to **E**, killer strains are indicated at the bottom of each panel. WT, wild type; Δ*vasK,* the T6SS-null

391   Δ*vasK* mutant; *4eff$_c$,* the 4-antibacterial-effector-inactive mutant; *tseH$^+$*, the TseH-active mutant. Survival of prey

392   cells was enumerated by serial plating on selective medium. Killer survival was shown in **Supplementary Figure**

393   **1A-1E** respectively. Error bars indicate the mean ± standard deviation of three biological replicates. Statistical

394   significance was calculated using a two-tailed Student's *t*-test for two groups comparison or one-way ANOVA

395   test for more than two groups comparison. ns, not significant; *, $p <0.05$; **, $p <0.01$; ***, $p< 0.001$; ****, $p<$

396   0.0001. DL, detection limit.

397   **Figure 2. Addition of Mg^{2+} and Ca^{2+} does not affect T6SS secretion. A,** Secretion analysis of Hcp in *V. cholerae*

398   strains with or without Mg^{2+} and Ca^{2+}. WT, wild type; Δ*vasK,* the T6SS-null Δ*vasK* mutant; *tseH$^+$*, the *tseH$^+$* only

399   mutant. (-), no cations addition; (+), addition of 0.27 mM Mg^{2+} and 0.07 mM Ca^{2+}. RpoB, the beta subunit of

400   DNA-directed RNA polymerase, serves as cell autolysis and loading control. Full images were shown in

401   **Supplementary Figure 2A**. **B,** Survival of the *Aeromonas dhakensis* SSU Δ*vasK* mutant after competition with

402   *V. cholerae* strains, as indicated. WT, wild type; Δ*vasK,* the T6SS-null Δ*vasK* mutant; *4eff$_c$,* the 4-antibacterial-

403   effector-inactive mutant; *tseH$^+$*, the TseH-active mutant. Survival of prey strains was enumerated by serial plating

404   on selective medium. Killer survival was shown in **Supplementary Figure 2B**. Error bars indicate the mean ±

405   standard deviation of three biological replicates. Statistical significance was calculated using a two-tailed Student's

406   *t*-test. ns, not significant; **, $p <0.01$. DL, detection limit.

407   **Figure 3. Innate immunity-like pathways protect *E. coli* against TseH. A**, Relative survival of *E. coli* strains

408   competed with the *V. cholerae 4eff$_c$* and *tseH$^+$* strain (*tseH$^+$/4eff$_c$*). WT, wild-type; Δ*phoQ*, the *phoQ* deletion

409   mutant; *phoQ^{D179L}*, a constitutively active *phoQ* mutant. Survival of prey strains were enumerated by serial plating

410 on selective medium. Killer survival was shown in **Supplementary Figure 3A**. **B**, Survival of *E. coli* ectopically

411 expressing TseH and its inactive mutant TseH^{H64A} with a periplasmic localization Tat signal. Cells were induced

412 with 0.1% [w/v] arabinose and survival was enumerated by serial plating on plates with 0.2% [w/v] glucose. **C**,

413 Volcano plot of RNA-seq results in *E. coli* samples ectopically expressing Tat-TseH and its inactive mutant Tat-

414 TseH^{H64A}. Differential expression genes were screened by setting cut-off value with fold change > 1.5, *p*-value <

415 0.05 and an average FPKM >10. Up and down-regulated genes were indicated in red and green, respectively.

416 Genes with no significant change were indicated in gray. **D**, Cluster analysis and heat map of differential expression

417 mRNAs in *E. coli* samples ectopically expressing Tat-TseH and its inactive mutant Tat-TseH^{H64A}. Scale means the

418 normalized FPKM of each sample by Z-score. **E**, qRT-PCR verification of differential expression of mRNA genes.

419 The 16S rRNA gene serves as the reference. For **A**, **B** and **E**, error bars indicate the mean ± standard deviation of

420 at least three biological replicates. Statistical significance was calculated using a two-tailed Student's *t*-test. *, *p*

421 <0.05; ****, *p*< 0.0001. DL, detection limit.

422 **Figure 4. Effects of cations and temperature on killing by other effectors. A,** Survival of *E. coli* after

423 competition with *V. cholerae* TseL-active mutant *tseL*$^+$ on LB source-1-agar or source-2-agar plates. **B,** Effect of

424 EDTA-treatment on survival of *E. coli* competed with *V. cholerae tseL*$^+$. The ddH$_2$O-treated agar plates serve as

425 control. **C,** Effect of cation supplementation on TseL-mediated *E. coli* killing. LB source-1-agar plates were

426 supplemented with 0.3 mM Ca^{2+}, Mg^{2+}, Cu^{2+} or Ni^{2+}, respectively. **D**, Relative survival of *E. coli* after competed

427 with *V. cholerae* strains at 30 ℃ or 37 ℃ (normalized to *4eff$_c$*), as indicated. For **A** to **D**, WT, wild type; *4eff$_c$*, the

428 4-antibacterial-effector-inactive mutant; *tseL*$^+$, the TseL-active only mutant. *vasX*$^+$, the VasX-active only mutant.

429 *vgrG3*$^+$, the VgrG3-active only mutant. Survival of *E. coli* strains was enumerated by serial plating on selective

430 medium. Survival of killer strains was shown in **Supplementary Figure 4A-4D**, respectively. **E**, Toxicity assay

431 of *P. aeruginosa* PAO1 strains ectopically expressing Tat-VasX and its colicin-inactivated mutant Tat-VasX$^{\Delta C16}$

432 on plates with gentamycin and irgasan at 30 ℃ or 37 ℃. For **A**-**E**, error bars indicate the mean ± standard

433 deviation of three biological replicates. Statistical significance was calculated using a two-tailed Student's *t*-test

434 for two groups comparison or one-way ANOVA test for more than two groups comparison. *, *p* <0.05; **, *p*

435 <0.01; ****, *p*< 0.0001. DL, detection limit.

436 **Figure 5. Competition analysis of TseH-mediated killing on raw agar. A**, Survival of *E. coli* prey competed

437 with *V. cholerae* strains on LB raw agar plates, as indicated. **B,** Survival of the *V. cholerae* Δ*tsiH* mutant as prey.

438 For **A** and **B**, killer strains are indicated at the bottom. WT, wild type; *4effc,* the 4-antibacterial-effector-inactive

439 mutant; *tseL*+, the TseL-active only mutant. Survival of prey cells was enumerated by serial plating on selective

440 medium. Killer survival was shown in **Supplementary Figure 5A**-**5B** respectively. Error bars indicate the mean

441 ± standard deviation of three biological replicates. Statistical significance was calculated using a two-tailed

442 Student's *t*-test. **, *p* <0.01; ****, *p*< 0.0001. DL, detection limit.

443 **Figure 6. Abiotic factors and stress response dictate the outcome of T6SS-mediated competition.**

444 Environmental abiotic factors affect the susceptibility of prey cells to T6SS effectors. These factors include the

445 presence metal cations, temperature, antibiotic molecules. Prey cells that do not possess specific immunity proteins

446 rely on innate immunity-like stress response pathways for protection. As an example, the PhoPQ two-component

447 system was activated under Mg^{2+}-limited environment, which is important for protecting *E. coli* from TseH-

448 mediated toxicity. Temperature and other environmental factors likely also modulate prey cell physiology to alter

449 cell sensitivity to T6SS-mediated competition. These abiotic factors thus play a key role in the dynamic

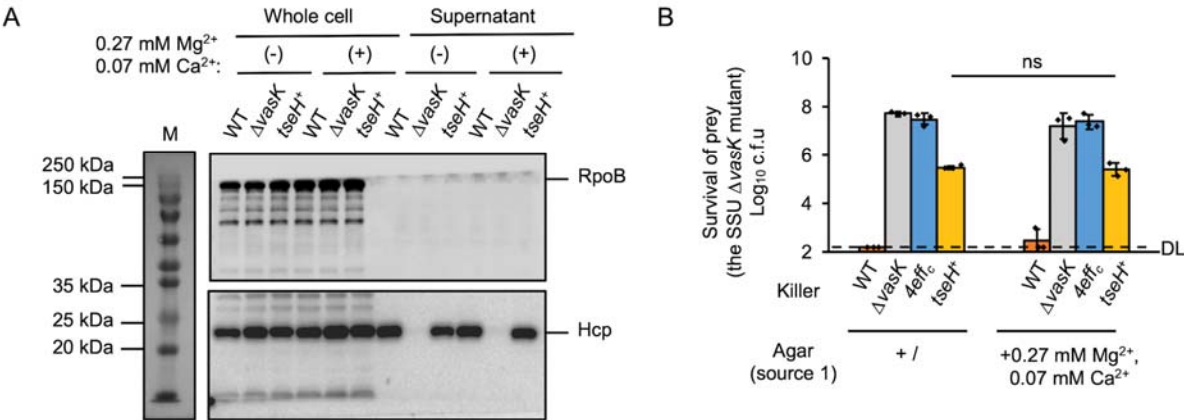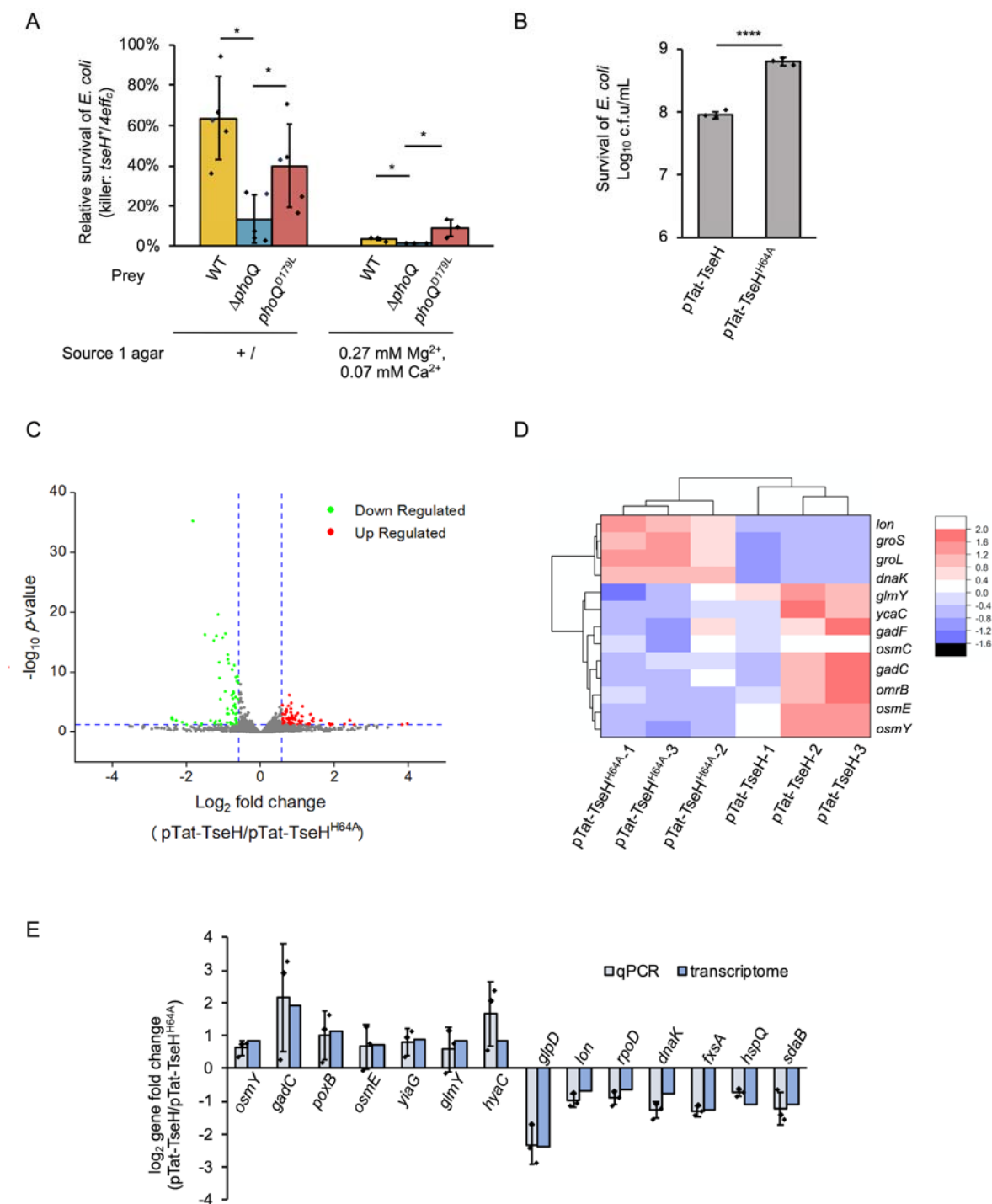450 competition of a T6SS-related microbial community.
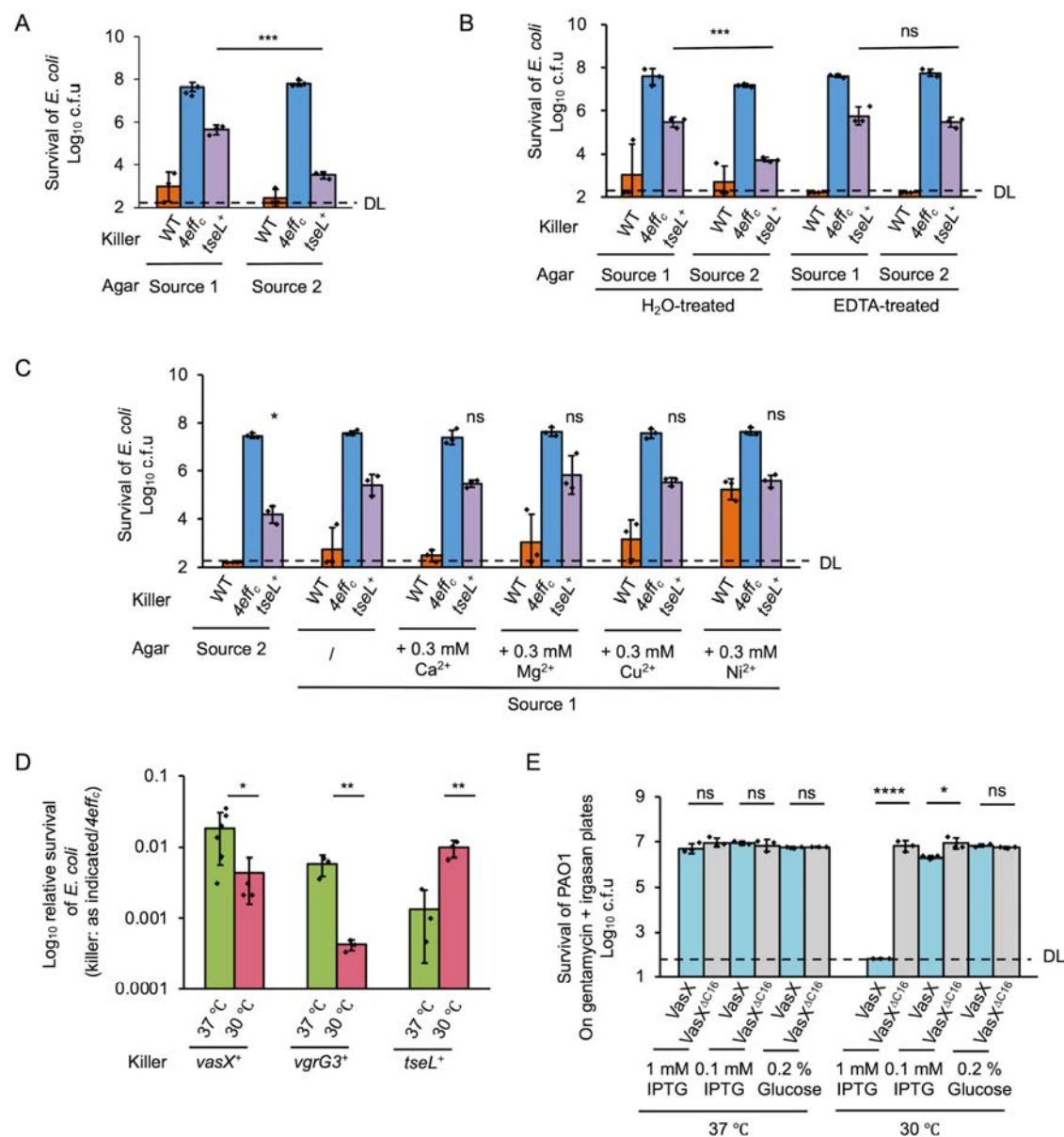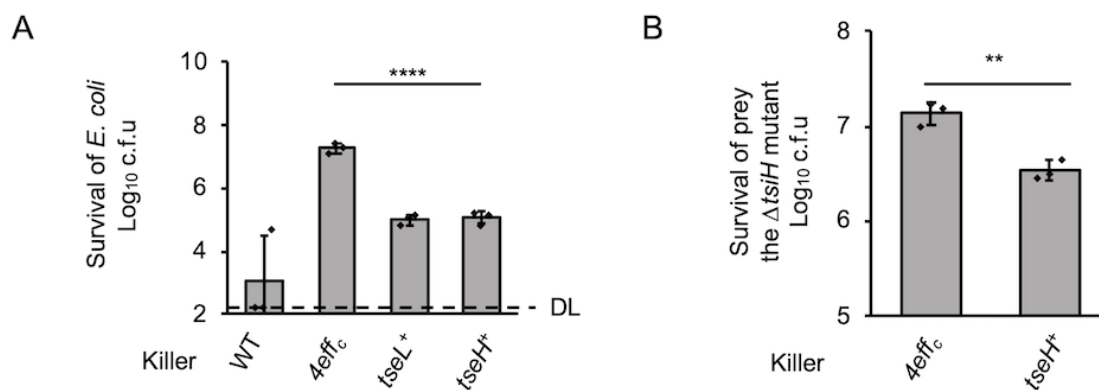
Figure 1
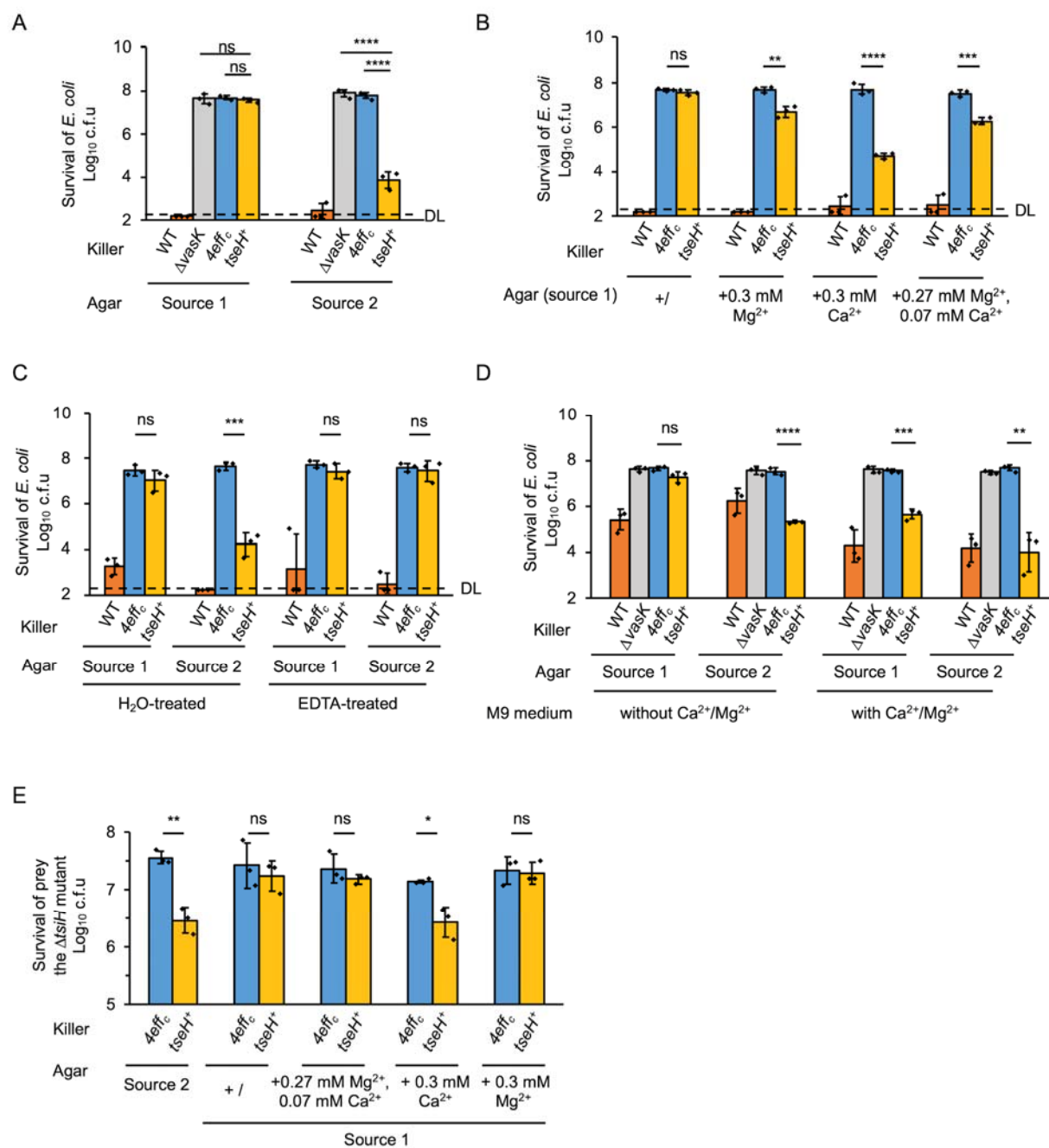
Figure 2

Figure 3

Figure 4

Figure 5

Figure 6